Identification of a mouse cytoskeleton-associated protein, CKAP2, with microtubule-stabilizing properties

Yi Jin,[1] Yoshiki Murakumo,[1,3] Kaoru Ueno,[1] Mizuo Hashimoto,[1] Tsuyoshi Watanabe,[1] Yoshie Shimoyama,[1] Masatoshi Ichihara[1] and Masahide Takahashi[1,2]

[1]Department of Pathology, Nagoya University Graduate School of Medicine, 65 Tsurumai-cho, Showa-ku, Nagoya 466-8550; and [2]Division of Molecular Pathology, Center for Neural Disease and Cancer, Nagoya University Graduate School of Medicine, 65 Tsurumai-cho, Showa-ku, Nagoya 466-8550

(Received July 14, 2004/Revised August 17, 2004/Accepted August 18, 2004)

Microtubule dynamics is an important factor in cell proliferation and one of the main targets of cancer chemotherapy. Since microtubule-associated proteins (MAPs) are known to influence microtubule stability, study of MAPs may contribute both to knowledge of cancer cell biology and to the production of new anti-cancer drugs. In this study, we identified a new mouse gene which is a homolog of human cytoskeleton-associated protein, *CKAP2* gene, by differential display analysis. The level of expression of mouse *CKAP2* (*mCKAP2*) was significantly higher in NIH3T3 cells expressing RET with a multiple endocrine neoplasia (*MEN) 2A* or *MEN2B* mutation than in parental NIH3T3 cells. Immunocytochemical analysis showed that mCKAP2 protein is localized in cytoplasm with a fibrillar appearance, and is co-localized with microtubules throughout the cell cycle. Furthermore, overexpression of mCKAP2 in cells appeared to stabilize microtubules against treatment with nocodazole, a microtubule-depolymerizing agent. In addition, levels of human CKAP2 were increased in some human tumor cell lines examined. These findings suggest that CKAP2 is a new MAP with microtubule-stabilizing properties and may represent a new molecular target for cancer chemotherapy. (Cancer Sci 2004; 95: 815–821)

Cell proliferation is closely associated with cytoskeleton organizing proteins, which play crucial roles in maintenance of cell structure, as well as mitotic progression. Of the three main filamentous components, microtubules, actin filaments and intermediate filaments, microtubules are known to play roles in intracellular organelle transport, cell division, and maintenance of cell morphogenesis.[1–3] Microtubules are composed of α- and β-tubulin proteins, and since their polymerization and depolymerization are essential for cell proliferation, various anti-cancer drugs have been produced to target microtubule dynamics and thereby inhibit mitotic progression. Some of these drugs inhibit microtubule polymerization, while others inhibit microtubule depolymerization.[3–5] Microtubule dynamics is regulated by accessory proteins called microtubule-associated proteins (MAPs).[6,7] Many proteins have been identified as MAPs, and can be generally classified into two categories, microtubule-stabilizing proteins and microtubule-destabilizing proteins. The former include tau, MAP2 and MAP4, while the latter include Op18/stathmin and heat shock protein HSP90.[8–13] Thus, characterization of the effects of MAPs on microtubule dynamics is necessary for investigation of the mechanisms of tumorigenesis and production of new anti-cancer drugs.

Neoplastic transformation of cells is triggered by genetic alterations which cause extraordinary cell growth and proliferation. A mutation in an oncogene can alter the function of its product, and the oncogenic signaling from the mutated protein can result in various neoplastic properties.[14,15] *RET* proto-oncogene encodes a transmembrane receptor with a tyrosine kinase domain which is expressed in cells derived from neural crest.[16–18] Glial cell line-derived neurotrophic factor (GDNF) activates RET, and the GDNF-RET signaling pathway plays an important role in the development of the enteric nervous system and the kidney.[19–22] Some mutations in *RET* result in activation of the RET protein, which induces neoplastic signaling and development of multiple endocrine neoplasia (MEN) type 2A and 2B.[23–26] MEN2A is characterized by the clinical features of medullary thyroid carcinoma (MTC), pheochromocytoma and parathyroid hyperplasia, while MEN2B is characterized by skeletal abnormalities and mucosal neuroma, as well as the features of MTC and pheochromocytoma. Mutations of *RET-MEN2A* are mainly observed at one of six cysteine residues in the extracellular cysteine-rich domain, while most *MEN2B* mutations are observed at a methionine residue of codon 918 in the intracellular kinase domain. The *MEN2A* type-mutated RET forms a homodimer by means of disulfide bond formation and is constitutively activated without ligand stimulation. The *MEN2B* mutation in RET may cause a conformational change in the intracellular kinase domain of RET, leading to its activation in a monomeric form.[27–29]

Here, we report the identification and characterization of a new mouse gene whose expression is induced by constitutively activated RET proteins. This gene was isolated by differential display analysis using NIH3T3 cells expressing the *MEN2A* or *MEN2B* type-mutated RET protein.[30] The transcript of this gene was more strongly expressed in NIH3T3 cells with mutated RET proteins than in parental NIH3T3 cells. Sequencing analysis showed that this gene is the mouse homolog of the human cytoskeleton-associated protein *CKAP2* gene (also termed *LB1*).[31–33] In addition, immunocytochemical staining suggested that this gene product is a microtubule-associated protein with microtubule stabilizing properties.

Materials and Methods

Cell culture and reagents. NIH3T3 cells expressing RET with *MEN2A* mutation (cysteine 634→arginine) or *MEN2B* mutation (methionine 918→threonine) and parental NIH3T3 cells were maintained in Dulbecco's modified Eagle's medium (DMEM) supplemented with 8% calf serum (Hyclone, Logan, UT).[34] For microtubule depolymerization analyses, cells were incubated in medium containing nocodazole (Sigma, St. Louis, MO).

[3]To whom correspondence should be addressed.
E-mail: murakumo@med.nagoya-u.ac.jp
The nucleotide sequence for the mouse CKAP2 gene has been deposited in the GenBank database under GenBank Accession Number AY692438.
Abbreviations: CKAP2, cytoskeleton-associated protein 2; MAP, microtubule-associated protein; MEN, multiple endocrine neoplasia; GDNF, glial cell line-derived neurotrophic factor; DD-PCR, differential display-polymerase chain reaction; RT, reverse transcriptase; GFP, green fluorescent protein; RACE, rapid amplification of cDNA ends; FITC, fluorescein isothiocyanate.

Differential display analysis. Total RNAs of NIH3T3, NIH3T3-RET (MEN2A) and NIH3T3-RET (MEN2B) cells were extracted using Trizol reagent (Invitrogen, Carlsbad, CA), and were treated with RNase-free DNase I to eliminate genomic DNA contamination. Differential display-polymerase chain reaction (DD-PCR) was performed using the TaKaRa rhodamine fluorescence differential display system according to the manufacturer's protocol (TaKaRa, Tokyo). The fluorescent products were subjected to electrophoresis on denaturing urea-4% polyacrylamide gels and visualized using FM-BIO II (TaKaRa). Differentially expressed products were extracted from the gels and amplified by PCR, and the amplified products were cloned into pGEM-T vector (Promega, Madison, WI). The cloned PCR products were subjected to sequencing.

Northern blot analysis. Ten microgram portions of total RNAs were subjected to electrophoresis on 1% agarose-formamide gels with formaldehyde and transferred onto Hybond-XL nylon membranes (Amersham Biosciences, Uppsala, Sweden). Northern hybridization was performed using radiolabelled probes of cDNA fragments identified by DD-PCR analysis.

Sequence determination of mouse *CKAP2* gene. An NIH3T3 cDNA phage library constructed in lambda ZAP II vectors (Stratagene, La Jolla, CA) was screened by conventional plaque hybridization using the radiolabelled probe of the cDNA fragment identified by DD-PCR analysis. The isolated positive phage clones were converted to plasmids according to the manufacturer's protocol (Stratagene). The plasmids were purified using a QIAGEN Plasmid Kit (Qiagen, Hilden, Germany) and subjected to sequencing. Double-strand DNA sequencing was performed by a cycle sequencing program using a BigDye Terminator Cycle Sequencing Kit (Applied Biosystems, Foster City, CA). Nucleotide sequences were determined by a Model 310 automated Applied Biosystems sequencer (Applied Biosystems). The sequences were confirmed by checking the products of 5′-rapid amplification of cDNA ends (RACE) and reverse transcriptase (RT)-PCR.

Construction of plasmids. Full-length mouse *CKAP2* (*mCKAP2*) cDNA was placed into the vector pcDNA3.1(+) (Invitrogen) with a FLAG sequence just before its ATG start codon (pcDNA3.1/FLAG-mCKAP2) in order to produce FLAG-tagged mCKAP2 protein in cells. Full-length *mCKAP2* cDNA was also placed into the vector pEGFP-C3 (Clontech, Palo Alto, CA) to express the mCKAP2 protein fused with green fluorescent protein (GFP) on its N-terminus (pEGFP/mCKAP2). In order to identify the tubulin association domain in mCKAP2 protein, the following truncated cDNA fragments of *mCKAP2* were subcloned into the vector pEGFP-C3 (fragment sizes are given in number of amino acids): aa 1–319, aa 309–664, aa 510–664, aa 1–159 and aa 160–319. The DNA fragment cloned into each vector was produced by PCR with *Pfu* DNA polymerase (Stratagene).

Transfection. For transient transfection, cells were transfected with the expression vectors indicated above using Lipofectamine 2000 transfection reagent according to the manufacturer's protocol (Invitrogen). The cells were used for analyses 48 h after transfection.

Antibodies. Mouse monoclonal anti-FLAG M2, anti-β-actin, anti-α-tubulin, anti-β-tubulin, anti-vimentin antibodies, Cy3-conjugated mouse monoclonal anti-β-tubulin antibody and rabbit polyclonal anti-FLAG antibody were purchased from Sigma.

Western blot analysis. Cells on 6 cm culture dishes were lysed in 500–1000 μl of 2× sample buffer (62.5 m*M* Tris-HCl pH 6.8, 2% SDS, 25% glycerol, 5% 2-mercaptoethanol, 0.01% bromophenol blue) with sonication. After boiling for 2 min, the lysates were subjected to SDS-polyacrylamide gel electrophoresis (SDS-PAGE) and transferred onto polyvinylidene difluoride membranes (Millipore, Bedford, MA). After blocking with 5% bovine serum albumin in TBST buffer (20 m*M* Tris-HCl pH 7.6, 137 m*M* NaCl, 0.1% Tween 20), the membranes were probed with anti-FLAG M2 antibody, followed by incubation with anti-mouse IgG secondary antibody conjugated to horseradish peroxidase (Dako, Kyoto, Japan). After intensive washing, the antigen-antibody complexes were visualized using the ECL Western blotting detection reagent (Amersham Biosciences).

Fluorescent immunostaining procedure. Cells grown on slide chambers (Becton Dickinson Labware, Bedford, MA) were rinsed twice with PBS and fixed by soaking in 100 % methanol at −20°C for 10 min, then permeabilized with 0.1% Triton X-100 in PBS. After blocking with 1% bovine serum albumin for 30 min, cells were incubated with a primary antibody for 1 h, followed by incubation with a secondary antibody conjugated with fluorescein isothiocyanate (FITC) or rhodamine for 30 min. After intensive washing, cells were examined with the FLUOVIEW FV500 confocal fluorescence microscope system (Olympus, Tokyo). For nuclear staining, cells were incubated with 0.5 μg/ml DAPI (Roche Diagnostics, Basel, Switzerland) for 10 min after incubation with secondary antibodies.

Statistical analysis for determination of microtubule stability. NIH3T3 cells with or without GFP-mCKAP2 expression were treated with 0.25 μg/ml of nocodazole for 20, 30 or 45 min, and were immunostained with Cy3-conjugated mouse monoclonal anti-β-tubulin antibody. More than 500 cells with GFP-mCKAP2 expression and more than 500 untransfected cells were counted under the fluorescence microscope, and the percentages of cells with microtubule fibrillar appearance were calculated. The difference in percentage of cells with such appearance between these groups was examined for significance by use of the χ^2 test.

Results

Cloning and expression of mouse *CKAP2* gene. We performed a DD-PCR analysis using RNAs isolated from parental NIH3T3 cells and NIH3T3 cells expressing RET-MEN2A or RET-MEN2B proteins (designated NIH3T3-RET (MEN2A) or NIH3T3-RET (MEN2B) cells). One DD-PCR product exhibiting lower expression in NIH3T3 cells and higher expression in NIH3T3-RET (MEN2A) and NIH3T3-RET (MEN2B) cells was identified (Fig. 1A). We cloned a complete cDNA 2304 bp in length from NIH3T3 cDNA phage library by using the cDNA fragment identified in DD-PCR analysis as a probe. The cDNA contained a 1995 bp ORF encoding a predicted protein of 664 amino acid residues with an expected molecular weight of 74 kDa. The sequence obtained was confirmed by 5′-RACE and RT-PCR. Homology search of the newly identified mouse gene revealed that its predicted amino acid sequence displayed significant homology with human cytoskeleton-associated protein, CKAP2. There was 62% amino acid identity between these two proteins (Fig. 1B). The expected protein sequence has no discernible domain structure. When we screened a human testis cDNA phage library using the mouse cDNA to identify the human homolog of this gene, we obtained four cDNA fragments of the human *CKAP2* gene (*hCKAP2*). We therefore concluded that the gene which we identified in the DD-PCR analysis is the mouse homolog of the human *CKAP2* gene (*mCKAP2*).

The genomic locus of *mCKAP2* is on mouse chromosome 8 and contains 9 exons covering a region of about 17 kb, according to the mouse genomic sequence in GenBank. Northern blot analysis of *mCKAP2* using a mouse Multiple Tissue Northern Blots membrane (Clontech) revealed a single band of about 2.4 kb with the highest expression in testis (Fig. 2A).

Localization of mCKAP2 in cells. We next examined the location of mCKAP2 protein in NIH3T3 cells. Because an antibody

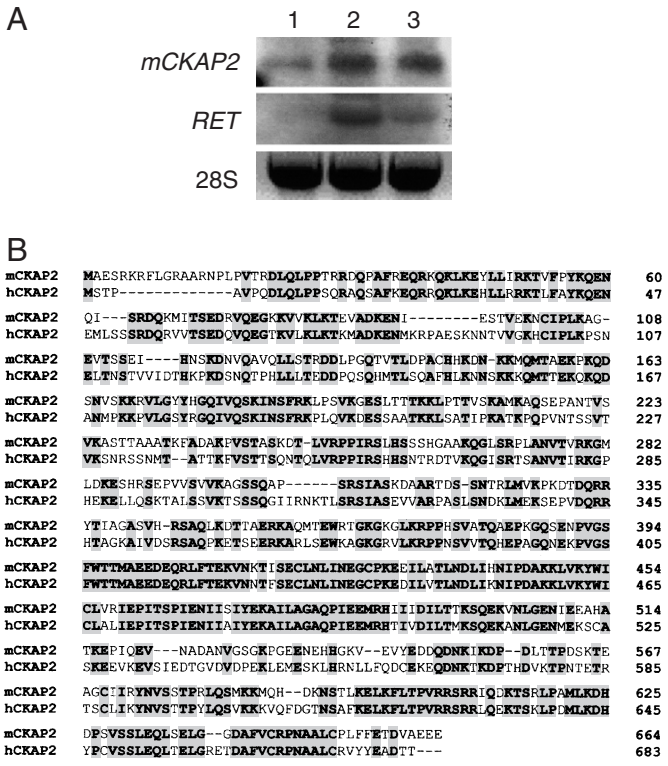

Fig. 1. *mCKAP2* transcript expression in NIH3T3, NIH3T3-RET (MEN2A) and NIH3T3-RET (MEN2B) cells, and amino acid sequence alignment of mCKAP2 with hCKAP2. A) Determination of *mCKAP2* expression by Northern blotting. The upper and middle panels show the blots probed by *mCKAP2* and *RET* cDNAs, respectively, while the lower panel shows 18S ribosomal RNA as a quantitative control. Lane 1, NIH3T3 RNA; lane 2, NIH3T3-RET (MEN2A) RNA; lane 3, NIH3T3-RET (MEN2B) RNA. B) Amino acid sequence alignment of mCKAP2 with hCKAP2. Amino acids identical in the two sequences are indicated in boldface. Dashes indicate gaps.

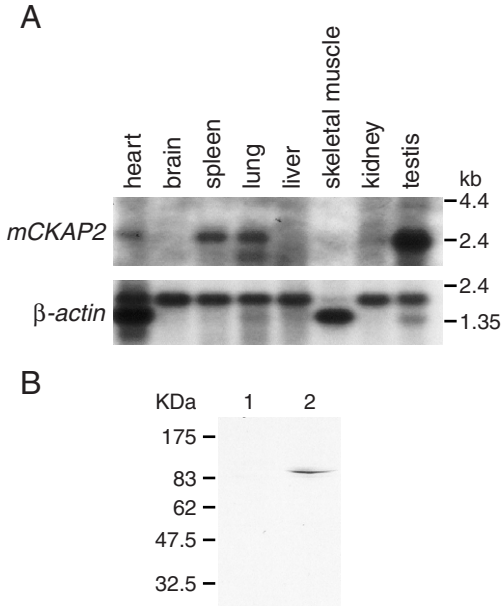

Fig. 2. Northern blot analysis of *mCKAP2* mRNA and Western blot analysis of FLAG-mCKAP2 protein. A) Northern blot analysis of *mCKAP2* mRNA expression in normal mouse tissues. The upper and lower panels show the blots probed by mouse *CKAP2* and *β-actin* cDNAs, respectively. B) Western blot analysis of FLAG-mCKAP2 protein. NIH3T3 cells transfected with pcDNA3.1/FLAG-mCKAP2 or pcDNA3.1(+) plasmids were disrupted in 2× sample buffer, and lysates were subjected to Western blotting with mouse monoclonal anti-FLAG antibody. Lanes 1 and 2 show the lysates of NIH3T3 cells transfected with pcDNA3.1(+) or with pcDNA3.1/FLAG-mCKAP2, respectively.

against mCKAP2 could not be obtained, we transfected pcDNA3.1/FLAG-mCKAP2 plasmids into NIH3T3 cells. Western blot analysis with anti-FLAG antibody revealed that FLAG-tagged mCKAP2 (FLAG-mCKAP2) protein was detected as a band of about 84 kDa (Fig. 2B). When the FLAG-mCKAP2 protein was immunostained 48 h after transfection, it was found to be distributed in cytoplasm with a fibrillar appearance in the transfected NIH3T3 cells (Fig. 3A, a, d). In some cells, the fibers appeared to spread from one center (Fig 3A, a, d). The same distribution of FLAG-mCKAP2 was observed in Cos-7, HEK293 and HeLa cells transfected with pcDNA3.1/FLAG-mCKAP2 plasmid (data not shown). Because the pattern of localization of FLAG-mCKAP2 was similar to those of proteins involved in cytoskeleton organization, we checked for co-localization of mCKAP2 protein with cytoskeleton organizing proteins, such as vimentin, β-actin and α- and β-tubulins. NIH3T3 cells transfected with the pcDNA3.1/FLAG-mCKAP2 plasmids were doubly immunostained using both rabbit polyclonal anti-FLAG antibody and mouse monoclonal anti-vimentin, anti-β-actin, anti-α-tubulin or anti-β-tubulin antibody, followed by reaction with FITC-conjugated anti-rabbit IgG and rhodamine-conjugated anti-mouse IgG secondary antibodies. FLAG-mCKAP2 protein was co-localized with α-tubulin (Fig. 3A, a–c) and β-tubulin (Fig. 3A, d–f) proteins forming microtubules and microtubule organizing centers, but not with vimentin or β-actin (data not shown).

When the transfected cells were incubated with 5 μg/ml of nocodazole, an inhibitor of microtubule polymerization, for 1 h, the fibrillar appearance of FLAG-mCKAP2 was lost, as also observed for tubulins (Fig. 3A, g–i). To confirm the mCKAP2 localization described above, we constructed another vector, pEGFP/mCKAP2, and NIH3T3 cells were transfected with it to produce GFP-fused mCKAP2 protein (GFP-mCKAP2). Transfected cells were immunostained with mouse monoclonal anti-α-tubulin antibody and rhodamine-conjugated anti-mouse IgG secondary antibody. Co-localization of GFP-mCKAP2 with α-tubulin was also observed (data not shown). Furthermore, co-localization of FLAG-mCKAP2 and α-tubulin was detected in the spindle and the midbody during the mitotic phase (Fig. 3B, e–l), indicating that mCKAP2 is a microtubule-associated protein.

Tubulin association domain in mCKAP2. To determine the tubulin association domain in mCKAP2, the truncated fragments of mCKAP2 cDNA (aa 1–319, aa 309–664, aa 510–664, aa 1–159 and aa 160–319) were subcloned into vector pEGFP-C3 and the corresponding GFP-fusion proteins were transiently expressed in NIH3T3 cells (Fig. 4A). GFP-fusion protein harboring the aa 1–319 or aa 160–319 mCKAP2 fragment exhibited a fibrillar appearance in cytoplasm, as did cells with the GFP-full-length-mCKAP2 protein, while the GFP-fusion protein harboring the aa 309–664, aa 510–664 or aa 1–159 fragment was diffusely distributed in cytoplasm without a fibrillar appearance (Fig. 4B). This finding indicated that the tubulin association domain in mCKAP2 resides within the region of amino acid residues 160 to 319.

mCKAP2 overexpression stabilizes microtubules against nocodazole treatment. Because it is known that some MAPs play roles in assuring microtubule stability against microtubule-depolymerizing agents, we investigated the effect of mCKAP2 overexpression on microtubule stability to nocodazole treatment. NIH3T3 cells transiently transfected with pEGFP/mCKAP2

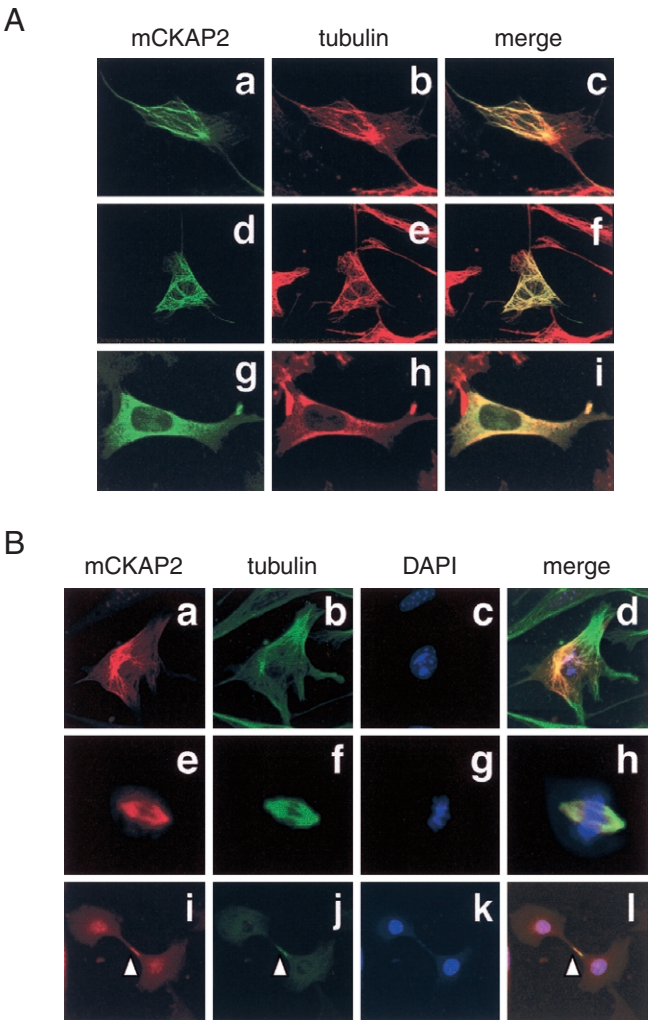

Fig. 3. Co-localization of mCKAP2 with microtubules. A) NIH3T3 cells transiently transfected with pcDNA3.1/FLAG-mCKAP2 were doubly immunostained with rabbit polyclonal anti-FLAG antibody and mouse monoclonal anti-α-tubulin antibody (a–c, g–i) or anti-β-tubulin antibody (d–f), followed by detection with FITC-conjugated anti-rabbit IgG secondary antibody and rhodamine-conjugated anti-mouse IgG secondary antibody. Cells were treated with 5 μg/ml nocodazole for 1 h before immunostaining (g–i). The left panels (a, d, g) show FLAG-mCKAP2 localization, while the middle panels (b, e, h) show α- or β-tubulin localization. Merged images are shown in the right panels (c, f, i). B) NIH3T3 cells transiently transfected with pcDNA3.1/FLAG-mCKAP2 were doubly immunostained with rabbit polyclonal anti-FLAG antibody and mouse monoclonal anti-α-tubulin antibody, followed by detection with rhodamine-conjugated anti-rabbit IgG secondary antibody and FITC-conjugated anti-mouse IgG secondary antibody. Nuclear staining with DAPI was performed after incubation with secondary antibodies. Cells in interphase (a–d), metaphase (e–h) and late telophase (i–l) are shown. The leftmost panels (a, e, i) show FLAG-mCKAP2 localization, the second panels (b, f, j) α-tubulin localization, the third panels (c, g, k) nuclear staining and the rightmost panels (d, h, l) show merged images. Arrowheads indicate the midbody.

plasmids were treated with 0.25 μg/ml of nocodazole for 20, 30 or 45 min, and were fixed and immunostained with Cy3-conjugated mouse monoclonal anti-β-tubulin antibody. As shown in Fig. 5, A and B, endogenous microtubule fibrillar appearance was hardly detected under these conditions. On the other hand, microtubules were quite stable to nocodazole treatment in NIH3T3 cells expressing GFP-mCKAP2 (Fig. 5A). Percentage expression of microtubule fibrillar appearance was

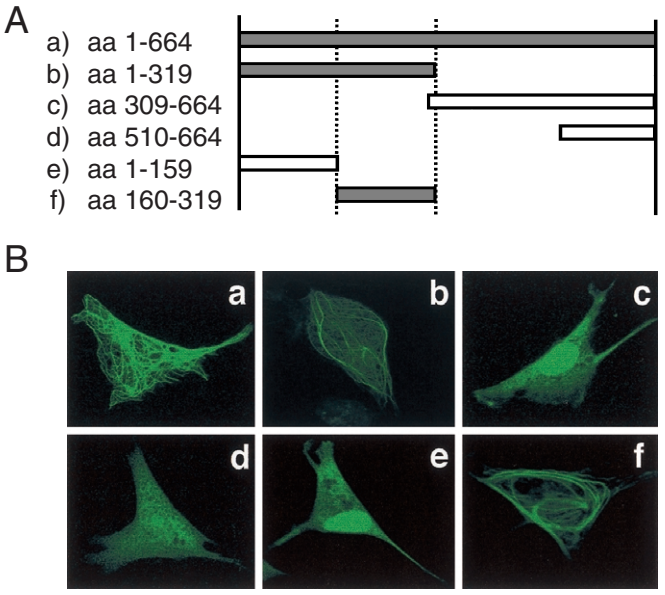

Fig. 4. Tubulin association domain in mCKAP2. A) The mCKAP2 fragments fused with GFP are illustrated. The amino acid (aa) numbers of the N- and C-termini of the fragments are indicated. The closed bars represent fragments whose GFP-fusion proteins exhibited fibrillar appearance in cytoplasm. B) Localization of the GFP-fusion mCKAP2 fragments in cells. Fibrillar appearance was observed for GFP-fusion fragments of aa 1–664 (a), aa 1–319 (b) and aa 160–319 (f), whereas diffuse distribution was observed for GFP-fusion fragments of aa 309–664 (c), aa 510–664 (d) and aa 1–150 (e).

significantly higher for cells expressing GFP-mCKAP2 than for cells without GFP-mCKAP2 expression at all time points examined (Fig. 5B). Similar findings of microtubule stability were observed when FLAG-mCKAP2 protein was transiently expressed in NIH3T3 cells (data not shown). This result suggested that mCKAP2 overexpression makes microtubules stable to nocodazole treatment, and that mCKAP2 might have microtubule-stabilizing properties.

***CKAP2* expression in human tumor cell lines.** Because it was reported that *hCKAP2* was expressed at high levels in human tumors such as hematopoietic tumors and gastric carcinomas,[31–33] we screened its expression in 26 human tumor cell lines by Northern blotting. *hCKAP2* expression was upregulated in some tumor cell lines, although the difference in its expression levels appeared to depend on individual cell lines rather than their histologic types. No alteration was observed in the size of the transcripts (Fig. 6).

Discussion

It is well-known that the homeostatic balance of proteins required for the maintenance of normal biological cell activities is lost in neoplastic cells as a result of oncogenic signaling. Many proteins, including growth factors and their receptors, signal transducers, and transcription factors, have been shown to participate in oncogenic signal pathways. Our aim is to identify the genes involved in oncogenic signal pathways associated with the mutated RET proteins which result in tumor development. In this paper, we have reported a new mouse gene exhibiting significant homology with the human *CKAP2* gene. The *hCKAP2* gene was originally identified as a gene highly expressed in diffuse large B cell lymphoma, and its product was subsequently reported as a cutaneous T-cell lymphoma-associated antigen.[31, 32] In addition, it was shown that this gene prod-

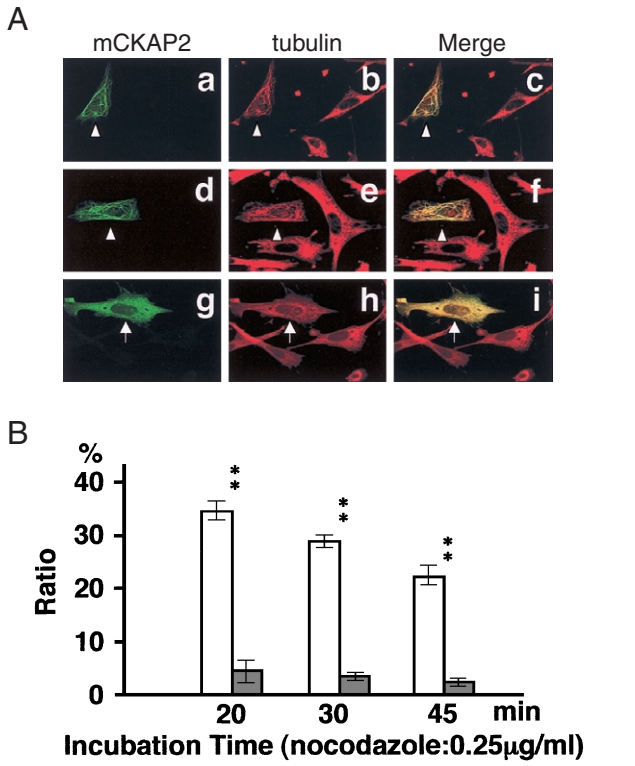

Fig. 5. mCKAP2 overexpression stabilizes microtubules against nocodazole treatment. NIH3T3 cells transiently transfected with pEGFP/mCKAP2 plasmids were treated with 0.25 μg/ml of nocodazole for 20, 30 or 45 min, and were immunostained with Cy3-conjugated anti-β-tubulin antibody. A) Examples of fluorescence microscopic images of cells with GFP-mCKAP2 expression (a–f) or GFP expression (g–i) and untransfected cells treated with nocodazole for 20 min. The left panels show GFP-mCKAP2 (a, d) or GFP (g) localization, the middle panels (b, e, h) β-tubulin localization, and the right panels (c, f, i) show merged images. Microtubule fibrillar appearance was observed in cells with GFP-mCKAP2 expression (indicated by arrowheads), while microtubule fibrillar appearance was not observed in cells with GFP expression (indicated by arrows) or untransfected cells. B) Percentages of cells with microtubule fibrillar appearance. More than 500 cells with GFP-mCKAP2 expression and more than 500 untransfected cells were counted under a fluorescence microscope, and the percentages of cells with microtubule fibrillar appearance were calculated. A significant difference in this percentage was observed between cells with GFP-mCKAP2 expression and untransfected cells at all time points observed (P **: <0.0001 by χ^2 test).

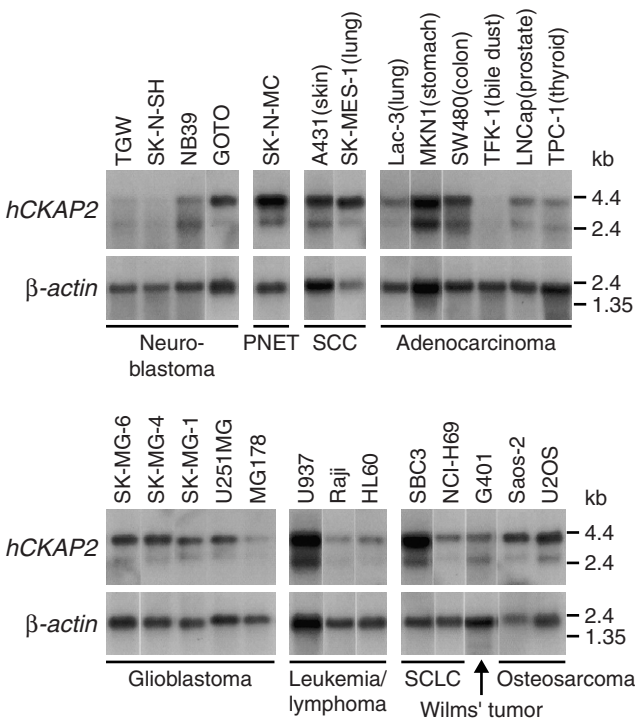

Fig. 6. Expression of human *CKAP2* mRNA in various human tumor cell lines. The upper and lower panels show the blots probed by human *CKAP2* and *β-actin* cDNAs, respectively. PNET, primitive neuroendocrine tumor; SCC, squamous cell carcinoma; SCLC, small cell lung carcinoma.

uct was located in cytoplasm with a filamentous pattern, indicating its association with cytoskeletal fibers. Recently, during preparation of this manuscript, Bae *et al*. reported that levels of CKAP2 are increased in primary human gastric adenocarcinomas and that hCKAP2 is co-localized with microtubules.[33] They suggested that hCKAP2 might be useful for discriminating adenocarcinomas from tubular adenomas.

We identified the mouse *CKAP2* gene in DD-PCR analysis using NIH3T3 cells and their derivatives, NIH3T3-RET (MEN2A) and NIH3T3-RET (MEN2B) cells. Expression of this gene was increased in the latter two cell types. These findings suggest the possibility that the *CKAP2* gene affects the biological properties of tumor cells. We recently reported that genes differentially expressed among NIH3T3-RET (MEN2A), NIH3T3-RET (MEN2B), and parental NIH3T3 cells can be classified into four categories; 1) those highly expressed in both NIH3T3-RET (MEN2A) and NIH3T3-RET (MEN2B) cells (type I); 2) those highly expressed in NIH3T3-RET (MEN2A) cells (type II); 3) those highly expressed in NIH3T3-RET (MEN2B) cells (type III); and 4) those highly expressed in parental NIH3T3 cells (type IV).[30] Type I included genes involved in cell growth, tumor progression and invasion, whereas type IV included genes implicated in tumor suppression. The pattern of expression of *mCKAP2* is consistent with that of type I genes. To further investigate whether or not *mCKAP2* expression is directly induced by mutated RET, we used MEF3T3 Tet-Off cells in which the gene expression is repressed by addition of tetracycline.[30] However, transient expression of the mutated RET protein did not significantly affect the level of *mCKAP2* expression (data not shown). In addition, we found that *hCKAP2* expression was not induced by GDNF stimulation (data not shown). Considering also the finding that hCKAP2 is upregulated in some human tumors, it is possible that *mCKAP2* expression was secondarily induced as a result of a constitutive tumorigenic signal by mutated RET protein.

The results of our immunocytochemical analyses showed that mCKAP2 protein is distributed in cytoplasm with a fibrillar appearance, and that mCKAP2 is co-localized with microtubules and microtubule organizing centers. Co-localization of mCKAP2 and microtubules was observed throughout the cell cycle. In addition, our findings suggested that mCKAP2 overexpression stabilized microtubules against treatment with the microtubule-depolymerizing agent nocodazole. Thus, it is possible that mCKAP2 is a microtubule-associated protein that functions as a microtubule stabilizer, like MAP2 and tau. Levels of MAP2 are reported to be increased in brain tumors, melanocytic tumors, pulmonary carcinoid tumors and small cell lung cancers, all of which are related to the nervous and neuroendocrine systems.[35–38] Expression of tau was observed in

tumors including astrocytomas, oligodendrogliomas, chondrosarcomas and gastrointestinal stromal tumors,[39–41] and tau phosphorylation is associated with anti-cancer drug sensitivity and drug-induced apoptosis.[42–45] We and other investigators found that expression of the *CKAP2* gene is also upregulated in some human tumors. Because some anti-cancer drugs target microtubule dynamics, the status of MAPs in cells might play a crucial role in determining the drug sensitivity of cancer cells. CKAP2 might thus prove useful as a target of cancer chemotherapy.

We thank Mr. Y. Imaizumi, Mr. K. Uchiyama, Miss M. Kozuka and Miss M. Kawai for technical assistance. This study was supported in part by Grants-in-aid for COE (Center Of Excellence) Research, Scientific Research (A) and Scientific Research on Priority Areas 'Cancer' from the Ministry of Education, Culture, Sports, Science and Technology of Japan, and by a Grant from Uehara Memorial Foundation.

1. Horwitz AR, Parsons JT. Cell migration—movin' on. *Science* 1999; **286**: 1102–3.
2. Rogers SL, Gelfand VI. Membrane trafficking, organelle transport, and the cytoskeleton. *Curr Opin Cell Biol* 2000; **12**: 57–62.
3. Valiron O, Caudron N, Job D. Microtubule dynamics. *Cell Mol Life Sci* 2001; **58**: 2069–84.
4. Downing KH. Structural basis for the interaction of tubulin with proteins and drugs that affect microtubule dynamics. *Annu Rev Cell Dev Biol* 2000; **16**: 89–111.
5. Checchi PM, Nettles JH, Zhou J, Snyder JP, Joshi HC. Microtubule-interacting drugs for cancer treatment. *Trends Pharmacol Sci* 2003; **24**: 361–5.
6. Drewes G, Ebneth A, Mandelkow EM. MAPs, MARKs and microtubule dynamics. *Trends Biochem Sci* 1998; **23**: 307–11.
7. Cassimeris L. Accessory protein regulation of microtubule dynamics throughout the cell cycle. *Curr Opin Cell Biol* 1999; **11**: 134–41.
8. Drechsel DN, Hyman AA, Cobb MH, Kirschner MW. Modulation of the dynamic instability of tubulin assembly by the microtubule-associated protein tau. *Mol Biol Cell* 1992; **3**: 1141–54.
9. Takemura R, Okabe S, Umeyama T, Kanai Y, Cowan NJ, Hirokawa N. Increased microtubule stability and alpha tubulin acetylation in cells transfected with microtubule-associated proteins MAP1B, MAP2 or tau. *J Cell Sci* 1992; **103**: 953–64.
10. Belmont LD, Mitchison TJ. Identification of a protein that interacts with tubulin dimers and increases the catastrophe rate of microtubules. *Cell* 1996; **84**: 623–31.
11. Marklund U, Larsson N, Gradin HM, Brattsand G, Gullberg M. Oncoprotein 18 is a phosphorylation-responsive regulator of microtubule dynamics. *EMBO J* 1996; **15**: 5290–8.
12. Nguyen HL, Chari S, Gruber D, Lue CM, Chapin SJ, Bulinski JC. Overexpression of full- or partial-length MAP4 stabilizes microtubules and alters cell growth. *J Cell Sci* 1997; **110**: 281–94.
13. Garnier C, Barbier P, Gilli R, Lopez C, Peyrot V, Briand C. Heat-shock protein 90 (hsp90) binds *in vitro* to tubulin dimer and inhibits microtubule formation. *Biochem Biophys Res Commun* 1998; **250**: 414–9.
14. Varmus HE. Viruses, genes, and cancer. I. The discovery of cellular oncogenes and their role in neoplasia *Cancer* 1985; **55**: 2324–8.
15. Polsky D, Cordon-Cardo C. Oncogenes in melanoma. *Oncogene* 2003; **22**: 3087–91.
16. Takahashi M, Ritz J, Cooper GM. Activation of a novel human transforming gene, *ret*, by DNA rearrangement. *Cell* 1985; **42**: 581–8.
17. Pachnis V, Mankoo B, Costantini F. Expression of the c-ret proto-oncogene during mouse embryogenesis. *Development* 1993; **119**: 1005–17.
18. Tsuzuki T, Takahashi M, Asai N, Iwashita T, Matsuyama M, Asai J. Spatial and temporal expression of the *ret* proto-oncogene product in embryonic, infant and adult rat tissues. *Oncogene* 1995; **10**: 191–8.
19. Schuchardt A, D'Agati V, Larsson-Blomberg L, Costantini F, Pachnis V. Defects in the kidney and enteric nervous system of mice lacking the tyrosine kinase receptor Ret. *Nature* 1994; **367**: 380–3.
20. Treanor JJ, Goodman L, de Sauvage F, Stone DM, Poulsen KT, Beck CD, Gray C, Armanini MP, Pollock RA, Hefti F, Phillips HS, Goddard A, Moore MW, Buj-Bello A, Davies AM, Asai N, Takahashi M, Vandlen R, Henderson CE, Rosenthal A. Characterization of a multicomponent receptor for GDNF. *Nature* 1996; **382**: 80–3.
21. Jing S, Wen D, Yu Y, Holst PL, Luo Y, Fang M, Tamir R, Antonio L, Hu Z, Cupples R, Louis JC, Hu S, Altrock BW, Fox GM. GDNF-induced activation of the ret protein tyrosine kinase is mediated by GDNFR-alpha, a novel receptor for GDNF. *Cell* 1996; **85**: 1113–24.
22. Takahashi M. The GDNF/RET signaling pathway and human diseases. *Cytokine Growth Factor Rev* 2001; **12**: 361–73.
23. Mulligan LM, Kwok JBJ, Healey CS, Elsdon MJ, Eng C, Gardner E, Love DR, Mole SE, Moore JK, Papi L, Ponder MA, Telenius H, Tunnacliffe A, Ponder BAJ. Germ-line mutations of the *RET* proto-oncogene in multiple endocrine neoplasia type 2A. *Nature* 1993; **363**: 458–60.
24. Donis-Keller H, Dou S, Chi D, Carlson KM, Toshima K, Lairmore TC, Howe JR, Moley JF, Goodfellow P, Wells SA Jr. Mutations in the RET proto-oncogene are associated with MEN 2A and FMTC. *Hum Mol Genet* 1993; **2**: 851–6.
25. Carlson KM, Dou S, Chi D, Scavarda N, Toshima K, Jackson CE, Wells SA Jr, Goodfellow PJ, Donis-Keller H. Single missense mutation in the tyrosine kinase catalytic domain of the *RET* protooncogene is associated with multiple endocrine neoplasia type 2B. *Proc Natl Acad Sci USA* 1994; **91**: 1579–83.
26. Hofstra RMW, Landsvater RM, Ceccherini I, Stulp RP, Stelwagen T, Luo Y, Pasini B, Hoppener JWM, Amstel HKPV, Romeo G, Lips CJM, Buys CHCM. A mutation in the *RET* proto-oncogene associated with multiple endocrine neoplasia type 2B and sporadic medullary thyroid carcinoma. *Nature* 1994; **367**: 375–6.
27. Santoro M, Carlomagno F, Romano A, Bottaro DP, Dathan NA, Grieco M, Fusco A, Vecchio G, Matoskova B, Kraus MH, Fiore PPD. Activation of *RET* as a dominant transforming gene by germline mutations of MEN2A and MEN2B. *Science* 1995; **267**: 381–3.
28. Asai N, Iwashita T, Matsuyama M, Takahashi M. Mechanism of activation of the *ret* proto-oncogene by multiple endocrine neoplasia 2A mutations. *Mol Cell Biol* 1995; **15**: 1613–9.
29. Borrello MG, Smith DP, Pasini B, Bongarzone I, Greco A, Lorenzo MJ, Arighi E, Miranda C, Eng C, Alberti L, Bocciardi R, Mondellini P, Scopsi L, Romeo G, Ponder BAJ, Pierotti MA. *RET* activation by germline *MEN2A* and *MEN2B* mutations. *Oncogene* 1995; **11**: 2419–27.
30. Watanabe T, Ichihara M, Hashimoto M, Shimono K, Shimoyama Y, Nagasaka T, Murakumo Y, Murakami H, Sugiura H, Iwata H, Ishiguro N, Takahashi M. Characterization of gene expression induced by RET with *MEN2A* or *MEN2B* mutation. *Am J Pathol* 2002; **161**: 249–56.
31. Maouche-Chretien L, Deleu N, Badoual C, Fraissignes P, Berger R, Gaulard P, Romeo PH, Leroy-Viard K. Identification of a novel cDNA, encoding a cytoskeletal associated protein, differentially expressed in diffuse large B cell lymphomas. *Oncogene* 1998; **17**: 1245–51.
32. Eichmuller S, Usener D, Dummer R, Stein A, Thiel D, Schadendorf D. Serological detection of cutaneous T-cell lymphoma-associated antigens. *Proc Natl Acad Sci USA* 2001; **98**: 629–34.
33. Bae CD, Sung YS, Jeon SM, Suh Y, Yang HK, Kim YI, Park KH, Choi J, Ahn G, Park J. Up-regulation of cytoskeletal-associated protein 2 in primary human gastric adenocarcinomas. *J Cancer Res Clin Oncol* 2003; **129**: 621–30.
34. Asai N, Murakami H, Iwashita T, Takahashi M. A mutation at tyrosine 1062 in MEN2A-Ret and MEN2B-Ret impairs their transforming activity and association with shc adaptor proteins. *J Biol Chem* 1996; **271**: 17644–9.
35. Fang D, Hallman J, Sangha N, Kute TE, Hammarback JA, White WL, Setaluri V. Expression of microtubule-associated protein 2 in benign and malignant melanocytes: implications for differentiation and progression of cutaneous melanoma. *Am J Pathol* 2001; **158**: 2107–15.
36. Liu Y, Sturgis CD, Grzybicki DM, Jasnosz KM, Olson PR, Tong M, Dabbs DD, Raab SS, Silverman JF. Microtubule-associated protein-2: a new sensitive and specific marker for pulmonary carcinoid tumor and small cell carcinoma. *Mod Pathol* 2001; **14**: 880–5.
37. Blumcke I, Becker AJ, Normann S, Hans V, Riederer BM, Krajewski S, Wiestler OD, Reifenberger G. Distinct expression pattern of microtubule-associated protein-2 in human oligodendrogliomas and glial precursor cells. *J Neuropathol Exp Neurol* 2001; **60**: 984–93.
38. Wharton SB, Chan KK, Whittle IR. Microtubule-associated protein 2 (MAP-2) is expressed in low and high grade diffuse astrocytomas, *J Clin Neurosci* 2002; **9**: 165–9.
39. Miyazono M, Iwaki T, Kitamoto T, Shin RW, Fukui M, Tateishi J. Widespread distribution of tau in the astrocytic elements of glial tumors. *Acta Neuropathol* 1993; **86**: 236–41.
40. Hu B, McPhaul L, Cornford M, Gaal K, Mirra J, French SW. Expression of tau proteins and tubulin in extraskeletal myxoid chondrosarcoma, chordoma, and other chondroid tumors. *Am J Clin Pathol* 1999; **112**: 189–93.
41. Chambonniere ML, Mosnier-Damet M, Mosnier JF. Expression of microtubule-associated protein tau by gastrointestinal stromal tumors. *Hum Pathol* 2001; **32**: 1166–73.
42. Sangrajrang S, Denoulet P, Millot G, Tatoud R, Podgorniak MP, Tew KD, Calvo F, Fellous A. Estramustine resistance correlates with tau over-expression in human prostatic carcinoma cells. *Int J Cancer* 1998; **77**: 626–31.
43. Veitia R, Bissery MC, Martinez C, Fellous A. Tau expression in model ade-

nocarcinomas correlates with docetaxel sensitivity in tumour-bearing mice. *Br J Cancer* 1998; **78**: 871–7.
44. Sangrajrang S, Calvo F, Fellous A. Estramustine resistance. *Gen Pharmacol* 1999; **33**: 107–13.
45. Guise S, Braguer D, Carles G, Delacourte A, Briand C. Hyperphosphorylation of tau is mediated by ERK activation during anticancer drug-induced apoptosis in neuroblastoma cells. *J Neurosci Res* 2001; **63**: 257–67.